

A MATHEMATICAL MODEL OF CREVICE AND PITTING CORROSION—I. THE PHYSICAL MODEL

S. M. SHARLAND and P. W. TASKER

Theoretical Physics Division, Harwell Laboratory, Oxfordshire OX11 0RA, U.K.

Abstract—A predictive and self-consistent mathematical model incorporating the electrochemical, chemical and ionic migration processes characterizing the propagation stage of crevice and pitting corrosion in metals is described. The model predicts the steady-state solution chemistry and electrode kinetics (and hence metal penetration rates) within an active corrosion cavity as a function of the many parameters on which these depend, such as external electrode potential and crevice dimensions. The crevice is modelled as a parallel-sided slot filled with a dilute sodium chloride solution. The cavity propagation rates are found to be faster in the case of a crevice with passive walls than one with active walls. The distribution of current over the internal surface of a crevice with corroding walls can be assessed using this model, giving an indication of the future shape of the cavity. The model is extended to include a solid hydroxide precipitation reaction and considers the effect of consequent changes in the chemical and physical environment within the crevice on the predicted corrosion rates. In this paper, the model is applied to crevice and pitting corrosion in carbon steel.

NOMENCLATURE

C_i	concentration of chemical species, i , mol dm ⁻³
D_i	diffusion coefficient of species i , m ² s ⁻¹
F	Faraday's constant of electrolysis, C mol ⁻¹
i	current density, A m ⁻²
k	chemical rate constant
K	equilibrium constant
l	length of crevice, m
R_g	molar gas constant, J mol ⁻¹ K ⁻¹
R_i	rate of production of species i by chemical reaction, mol s ⁻¹
T	temperature, K
U_i	mobility of species, m ² mol J ⁻¹ s ⁻¹
w	width of crevice, m
z_i	charge number of species i
α	electrochemical partition coefficient
ϕ	electrostatic potential drop in crevice, V
ϕ_M	electrostatic potential of corroding metal, V
σ	charge density, C m ⁻³

INTRODUCTION

A PASSIVE metal surface exposed to a corrosive environment may experience attack at several isolated sites. If the total area of these sites is small compared with the whole surface area, then the metal is said to be experiencing localized corrosion. The rate of metal dissolution in this situation is often much greater than that associated with uniform corrosion and structural failure may occur in a very short period. Several different modes of localized corrosion may be identified and are dependent

on the type of metal undergoing corrosion and its physical and chemical environment at the time of attack. One of the most familiar is pitting corrosion which is characterized by the presence of a number of small, roughly hemispherical cavities on the exposed surface. The geometries of these pits depend on many factors such as the metal composition and the surface orientation. A similar mode of corrosion is crevice attack which occurs where there are two or more surfaces in close proximity, leading to the creation of a locally occluded region where enhanced dissolution may occur. There are many mechanistic similarities associated with the growth of established pits and crevices. Other types of localized corrosion include stress-corrosion cracking, corrosion fatigue cracking and intergranular attack but these will not be considered here.

The rapidity with which localized corrosion can lead to the failure of a metal structure has led to a great deal of study of this phenomenon. There are many difficulties associated with the experimental measurement of the electrochemical conditions within cavities and as a result a number of mathematical models have been developed. The aim of this paper is to present a model of the propagation of an active corrosion crevice or pit which is entirely predictive and self-consistent, using a series of physically based approximations and assumptions. The model predicts the steady-state solution chemistry and electrochemistry (and hence metal penetration rates) within the restricted geometries of the cavities. The input parameters of the model describe the physical and chemical environment of the crevice, e.g. metal potential, pH of the electrolyte etc. The model also uses empirically determined electrode reaction rates. It is developed in a number of distinct stages, each considering an additional physical process or chemical equilibrium reaction. The related mathematical additions, justification of approximations and methods of solution at each stage are described fully in an accompanying paper. It is not intended to present a detailed comparison of the predictions of the model with experimental results in this paper, but more general assessments of the accuracy of the model will be made by considering the order of magnitudes of the predicted cavity propagation rates and qualitative variation in these with the parameters of the system. In this way, the importance of some of the approximations and empirical input data to the predictions of the model may be determined. A more detailed model validation will be carried out at a later stage. In this paper, input data appropriate to the corrosion of carbon steel are used, although the model may be applied to a wide range of metals. (It has been shown experimentally that carbon steel will passivate (and be susceptible to pitting or crevice corrosion) in a wide range of solutions containing chloride ions¹).

In the first section, the mathematical description of an active crevice or pit is discussed. These methods will be compared with several models of the solution chemistry and electrochemistry within corroding cavities from the literature. In the following section, details of a simple model of a crevice which is corroding only at the base and includes only one hydrolysis reaction are outlined. The walls of this cavity are assumed passive, allowing a simplified description of the ionic migration processes within the cavity. This model is then extended to a more realistic description of an established localized corrosion site and it is assumed that corrosion occurs on the crevice walls also. The predictions from both models are then discussed and compared. In particular, the distribution of current on the walls is considered and the effect of passivation on parts of the walls, giving an indication of the future shape of the cavity.

Precipitation of solid hydroxide is monitored in both these models by checking the concentrations for appropriate excesses above the solubility limit of the solid. In the next section, the active and passive wall models are extended to include the precipitation reaction directly. The kinetics of the precipitation are assumed to be rapid compared with the migration processes and the ionic concentrations are constrained by the equilibria relation for the precipitation reaction. The results are compared with those from a crevice with no solid present. The sensitivity of the predictions to the diffusion coefficient in the crevice (reduced by the presence of the solid corrosion product) is tested. In the final section, limitations of the models and possible extensions to improve agreement with experiment are discussed.

MATHEMATICAL DESCRIPTION OF CREVICE AND PIT PROPAGATION

The chemical environment within a localized corrosion cavity is often very different from that outside. The common aim of the mathematical models that are described here is the prediction of the solution chemistry and electrochemistry within the restricted geometries of the cavities as a function of the many physical and chemical parameters of the system, such as crevice dimensions and bulk solution composition. Such information yields metal penetration rates. A full description of the problem should include an account of the complex solution chemistry within the crevice, the electrochemical reaction rates and their dependence on parameters such as electrostatic potential and solution pH, the migration of ions under both concentration and potential gradients, the advection of ions in flowing electrolytes, the effect of the changing shape and dimensions of the crevice as propagation proceeds and the effect of the blocking of the crevice with solid corrosion product. These processes are schematically illustrated in Fig. 1.

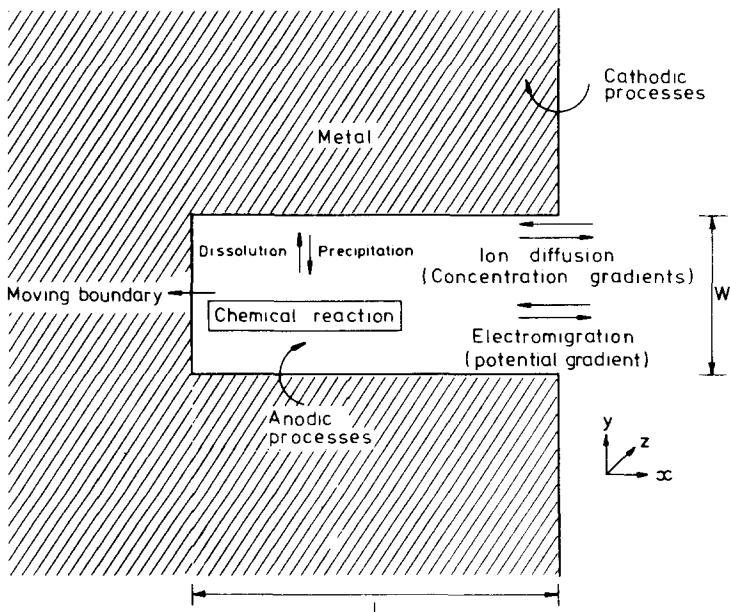


FIG. 1. Schematic illustration of the crevice of pit model.

The mathematical model of cavity propagation is based on the set of fundamental equations governing the mass transport of aqueous chemical species in dilute electrolytic solutions. The concentration of chemical species i , C_i obeys the following mass-conservation equation (assuming the electrolyte is static),

$$\frac{\partial C_i}{\partial t} = D_i \nabla^2 C_i + z_i U_i \nabla(C_i \nabla \phi) + R_i. \quad (1)$$

D_i is the effective diffusion coefficient of species i , z_i the charge number, ϕ is the electrostatic potential in the solution, R_i represents the rate of production or depletion of species i by chemical reaction and U_i is the mobility, given by the expression

$$U_i = \frac{D_i}{RT}. \quad (2)$$

The first term on the right-hand side of the equation represents the contribution to the overall transport rate from ionic diffusion and the second term is the contribution by electromigration for the charged species. The electrostatic potential of the system, ϕ is governed by Poisson's equation,

$$\nabla^2 \phi = \frac{\sigma}{\epsilon}, \quad (3)$$

where σ is the charge density and ϵ is the permittivity of the electrolyte. For water ϵ is 80, and the magnitude of ϵ^{-1} is sufficiently large that any departure of the system from electroneutrality results in a very large electrical restoring force. This force tends to remove charge gradients on a much faster timescale than those associated with the diffusion processes. As an approximation therefore, Poisson's equation is often replaced by the equation of local charge neutrality

$$\sum_i z_i C_i(x) = 0 \quad (4)$$

for all x in the crevice. The boundary conditions of the problem are as follows:

(1) The concentrations of the species are fixed at the cavity mouth and are equal to the values in the bulk solution outside the corrosion site.

(2) The flux of species either produced or consumed in the electrode processes are proportional to the corresponding electrochemical reaction rates on the crevice walls. The fluxes of the other species at the walls are zero.

Solutions of the problem have been obtained using a variety of approximations to the equations themselves, the boundary conditions and the geometry of the crevice. The most common approximations are as follows:

(1) Adoption of simplified geometries representing the pit or crevice.

(2) Reduction of the number of dimensions of the problem, usually to one, for example, by assuming that the behaviour of the cavity is dominated by chemical variations along the direction perpendicular to the outer metal surface or that the cavity walls are passive.

(3) Neglect of diffusion of ionic species under concentration gradients.

(4) Neglect of migration of charged species under potential gradients.

(5) Neglect of convection of species by a moving electrolyte.

(6) Neglect of the effects of the retreating walls of the cavity, i.e. the convected electrolyte and the lengthening of the migration paths of the species.

(7) Simplification of the chemistry and electrochemistry by consideration of a small number of chemical species and a limited number of equilibria and electrode reactions.

(8) Neglect of the dependence of electrochemical reaction rates on solution chemistry and electrochemistry within the crevice.

(9) Assumption of the steady state.

The simplest models consider ionic migration by one transport mode only, but these are only strictly applicable to fairly narrow ranges of timescales and environments. For example, models which neglect ionic diffusion are only valid at short times since any increase in electrostatic potential in the cavity implies some imbalance in ionic concentrations and subsequent diffusion. Similarly, models which neglect electromigration are also restricted; they are either specific to some experimental system in which the potential gradients have been shown to be small over the relevant timescales or they consider only the transport of a neutral species. The more general models are those which consider diffusion and electromigration (and convection for situations in which the electrolyte is flowing). There have been a number of such models reported in the literature.

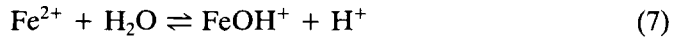
Some of the methods used in two literature models (Turnbull *et al.*²⁻³ and Galvele *et al.*⁴⁻⁶) are now compared and the importance of some of the assumptions and approximations to the general accuracy of the predictions are discussed. These models involve a parallel-sided corroding cavity and yield a steady-state solution for the chemistry and electrochemistry although the applications of the models do differ. Both models consider diffusion, electromigration and chemical reaction of at least six aqueous species within the cavity. This is the minimum number necessary to simulate the behaviour of a localized corrosion site. These species are metal ions from the dissolution process (Me^{z+}), hydroxyl and hydrogen ions from the water dissociation (OH^- and H^+), a metal hydrolysis product ($\text{MeOH}^{(z-1)+}$ as the simplest) and sodium and chloride ions to facilitate current flow within the crevice. Both models include some buffering reactions to obtain more realistic simulation of particular experimental systems. However there are a number of differences; Galvele considers a cavity with passive walls, whereas Turnbull includes the effect of corrosion on the walls. Also, there are differences in the approximations made to the boundary conditions of the problem and in the range of parameters over which each model is applied. The models of Turnbull are applied to conditions of cathodic control [for metals polarized to potentials less than about -0.5 V(SCE)]. The anodic dissolution of the metal is assumed to follow Tafel kinetics, i.e. the dissolution current is assumed to obey the following equation,

$$i = i_0 \exp(-\alpha E/RT), \quad (5)$$

with E the electrode potential and the parameters i_0 and α obtained from polarization experiments. Two cathodic reactions are considered in this model; the reduction of water (also assumed to obey Tafel kinetics) and the reduction of hydrogen ions. The rate of the latter reaction is assumed to depend linearly on the pH, i.e.

$$i = i_0[\text{H}^+] \exp(-\alpha E/RT). \quad (6)$$

Only one metal hydrolysis reaction is included,



since no hydroxide is assumed to precipitate at low metal potentials.

In the models of Galvele *et al.*, the cathodic reactions within the crevice are neglected. This approximation limits the range of application to higher metal potentials. This consideration of only one electrode reaction alleviates the need to consider a direct relationship between the current and electrode potential. If, however, the kinetics of the anodic dissolution reaction are assumed, this model effectively yields the potential of the metal as a function of the corrosion current density, whereas the model of Turnbull can be used to predict the current from the metal potential. The model of Galvele also includes the precipitation of a solid ferrous hydroxide, since at higher metal potentials the predicted ionic concentrations exceed the solubility product of this phase. The solid is treated as a mobile species and the appropriate mass-balance equation is derived and solved. The hydroxide is assumed to be precipitated as colloidal particles and not to influence the migration of other mobile species (through scaling of the diffusion coefficients, for example). This model may be regarded, therefore, as representing the very early stages of precipitation in a corroding device.

The predictions of both models have been compared with various experiments. Turnbull compared results from his model with measured potentials and pH values in an artificial crevice. He obtains good qualitative agreement with experimental data but both the predicted hydrogen ion concentration and the potential drop in the cavity are somewhat lower than measured experimental results. Although no measurements of the cavity propagation rates are given, so no direct comparison may be made, this would suggest that the predicted rates are higher than in reality. Galvele tested his model by comparing a calculated pitting potential against experiment. The agreement was found to be good for a number of different solution compositions. However, if the metal potential associated with a particular current density is calculated, using the predicted solution potential in the model (assuming the kinetics of the dissolution reaction) the cavity propagation rate is found to be faster than reasonably expected for such a polarization. Turnbull suggests that the inaccuracy in some of his predictions arises chiefly from the assumption of no solid phases in the crevice and suggests that at such low potentials magnetite (Fe_3O_4) would be the stable phase. Galvele includes the solid phase in his model and still predicts high corrosion rates. However, a cavity with passive walls is assumed in this case and it will be shown that corrosion of the walls in a real system increases the potential drop in the cavity, thus reducing the corrosion current.

DETAILED DESCRIPTION OF MODEL OF PROPAGATION OF CORROSION CAVITY

The pit or crevice is modelled as a parallel-sided slot of length l , width w , and thickness d (Fig. 1). The crevice is assumed to be filled with a dilute aggressive solution, in this case NaCl, initially at concentration 10^{-3} mol dm^{-3} . The following assumptions are made:

(1) The metal surface outside the crevice is assumed covered with a passive film and there is sufficient generation of cathodic charge on the outer surface to drive localized corrosion.

(2) The surface area of the slot is very much smaller than the surface area of the metal and changes in conditions in the cavity do not affect the potential of the whole specimen.

(3) The thickness of the slot, d is very much larger than the length, l and thus transport on the z direction may be neglected.

(4) The electrolyte is static.

(5) Cavity propagation is slow compared with ionic migration rate and both the moving boundary and any induced electrolyte motion may be ignored.

(6) The crevice solution is anaerobic.

(7) Dilute solution theory is used throughout and the activity of water is not considered specifically.

In our model, the following electrochemical reactions and kinetics are assumed. For the oxidation of iron



Turnbull and Gardner⁷ found that between pH 3 and 8.5, an expression of the form

$$i_1 = i_{01} \exp [\alpha_1 FE/R_g T], \quad (9)$$

with $i_{01} = 2.7 \times 10^{11} \text{ A m}^{-2}$ and $\alpha_1 = 1$ describes the current quite accurately. E is the electrode potential measured on the SCE scale. The reduction of water



was found by Turnbull and Thomas³ to follow the relationship

$$i_2 = i_{02} \exp [\alpha_2 FE/R_g T], \quad (11)$$

with i_{02} and α_2 independent of pH below values of 10 and taking values $-8 \times 10^{-10} \text{ A m}^{-2}$ and -0.5 , respectively. The hydrogen discharge reaction



was found by Turnbull and Thomas³ to show a first order dependence on hydrogen ion concentration

$$i_3 = i_{03}[\text{H}^+] \exp [\alpha_3 FE/R_g T], \quad (13)$$

with $i_{03} = 2 \times 10^{-4} \text{ A mole}^{-1} \text{ dm}^3 \text{ m}^{-2}$ and $\alpha_3 = -0.5$.

Initially two chemical reactions are considered in the model:



The first reaction is simplified from the many-stage hydrolysis that is likely to occur.⁶ This simplification is quite reasonable since the chemical reactions are much faster than the diffusion processes so that the detailed kinetics of several parallel reaction schemes can be collected into one overall scheme: it is only the equilibrium constant which really matters, and this is determined by the free energies of the species. Thus any simplifications here are likely to have less effect on the results than the simplifications made in the electrode kinetics.

The equilibrium constants of the reactions K_1 and K_2 calculated using

$$R_g T \ln K_1 = G_f(\text{Fe}^{2+}) + G_f(\text{H}_2\text{O}) - G_f(\text{FeOH}^+) - G_f(\text{H}^+)$$

TABLE 1. GIBBS FREE ENERGIES OF FORMATION OF SPECIES

Species	Free energy kJ mol ⁻¹
Fe ²⁺	-78.87
FeOH ⁺	-277.3
Fe(OH) ₂ (s)	-488.6
H ₂ O	-237.18
H ⁺	0.0
OH ⁻	-157.3

and

$$R_g T \ln K_2 = G_f(\text{H}^+) + G_f(\text{OH}^-) - G_f(\text{H}_2\text{O})$$

where $G_f(S)$ is the Gibbs free energy of formation of species S , given in Table 1. The individual forward and backward reaction rates are denoted k_{1F} , k_{1B} and k_{2F} , k_{2B} where

$$K_1 = \frac{k_{1F}}{k_{1B}}, \quad K_2 = \frac{k_{2F}}{k_{2B}}.$$

The sodium and chloride ions are assumed not to take part in the chemical reactions but contribute to the transfer of current within the crevice.

In the model, it is first assumed that the crevice walls are passive, so the steady-state mass-conservation equations for the aqueous chemical species become

$$D_i \left[\frac{d^2 C_i}{dx^2} + \frac{z_i}{R_g T} \frac{d}{dx} \left(C_i \frac{d\phi}{dx} \right) \right] + R_i = 0. \quad (16)$$

The six equations and the boundary conditions at the crevice tip and mouth are specified fully in the accompanying paper.

The equations describing corrosion in two directions are derived in a similar manner, i.e. with the electrode processes occurring on the crevice walls in addition to the crevice tip. An approximation derived by Turnbull⁸ which averages the contributions from the walls across the width of the crevice, assuming a uniform transverse concentration profile, is used. This effectively adds a term involving the potential- (and hence position-) dependent currents and crevice width to the right hand side of the mass-balance equations of the species involved in electrode processes. The boundary conditions for this set of coupled differential equations are as before. These equations are also given in the accompanying paper.⁹

Numerical solution

An analytical solution of the two sets of equations would be extremely difficult since they are highly non-linear in nature. The non-linearity arises from the dependence of the flux boundary condition at the crevice tip on the electrode potential, which is one of the unknown variables of the system. However, by transforming to dimensionless coordinates, rearranging and integrating, a form suitable for numerical integration may be obtained. Full details of this method are given in the accompanying paper.⁹ However, in brief, solution of the equations involved making

an initial guess at the potential and pH profiles, calculating the various parameters dependent on these, solving the coupled equations and comparing the resultant potential and pH distributions with the estimates. If these did not coincide then the calculated profiles were used for the next iteration. This process was continued until convergence and hence a self-consistent solution was reached. The subroutine chosen for the solution of the system was a variable-order, backward-differentiation formula method known as Gear's method. Several techniques involving a variety of mathematical approximations which reduce computing time have been developed for solution of this system of equations. These are described in the numerical methods section of the accompanying paper.

CALCULATED RESULTS

The electrode kinetic and chemical equilibria parameters have been described previously. The diffusion coefficients of all species except H^+ and OH^- are taken as $1 \times 10^{-9} \text{ m}^2 \text{ s}^{-1}$. The diffusion coefficient of H^+ is assumed $9.3 \times 10^{-9} \text{ m}^2 \text{ s}^{-1}$ and of OH^- $5.3 \times 10^{-9} \text{ m}^2 \text{ s}^{-1}$. Initially a crevice of length 2 mm and width $10 \mu\text{m}$ in a neutral solution of NaCl of strength 10^{-3} M is considered. The temperature is assumed to be 25°C .

Firstly, a crevice with passive walls was considered. Figure 2 shows details of the solution chemistry for a metal potential of -0.2 V . The pH of the solution decreases rapidly near the crevice mouth from a bulk value of 7 to about 4 and then decreases slowly to a value of 3.4 at the crevice tip. Large quantities of Fe^{2+} are generated with concentrations reaching more than 10 M at the crack tip. (At such high concentrations the assumption of dilute solution theory is not valid.) The chloride ion concentration also increases rapidly with distance along the crevice ensuring charge neutrality is maintained everywhere. Figure 3 shows the chemistry for a metal at potential 0.0 V . The $[Cl^-]$ and $[Fe^{2+}]$ rise and pH drop along the pit are more significant for higher potentials. Figure 4 shows a comparison of the potential drops

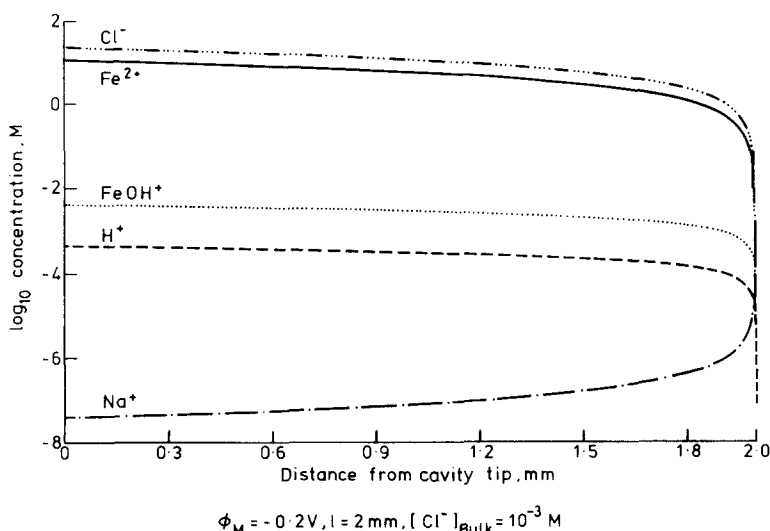


FIG. 2. Concentration profiles along the cavity length for a crevice with passive walls.

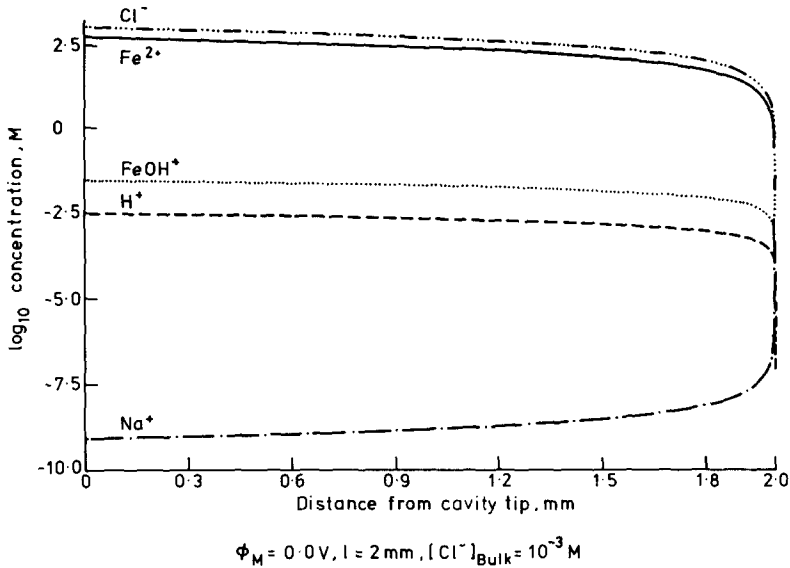


FIG. 3. Concentration profiles along the cavity length for a crevice with passive walls.

along the cavity length for metals at potentials -0.4 , -0.2 and 0.0 V . The calculated corrosion currents associated with these electrode potentials are extremely high under these theoretical conditions. It will be shown that inclusion of corrosion on the cavity walls reduces the corrosion current densities considerably. Figure 5 shows the variation of corrosion current with cavity length (with each calculation carried out independently in a static geometry, i.e. no moving boundaries are involved here) for the case $\phi_M = -0.2 \text{ V}$. Although the magnitudes of the currents are physically unrealistic (for reasons which will be suggested later), the general trend of decreasing current with increasing diffusion length is significant.

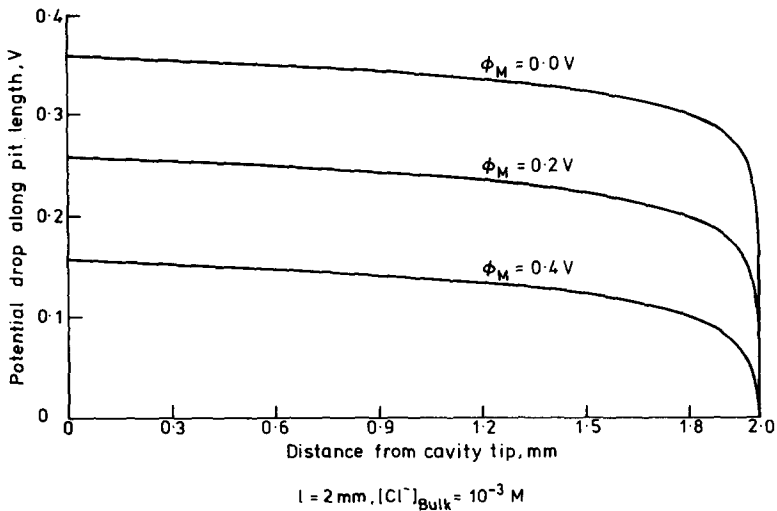


FIG. 4. Electrostatic potential drop along cavity length for a crevice with passive walls.

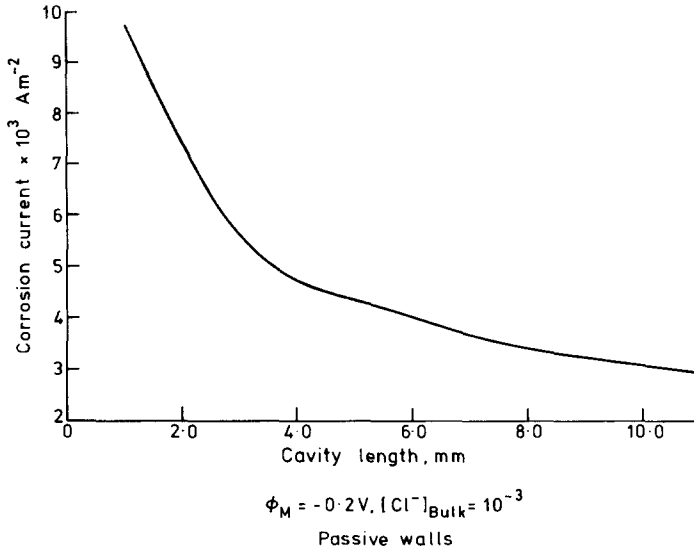


FIG. 5. Corrosion current against cavity length.

The model includes an account of cathodic reactions occurring at the pit base. However, these currents are very small at such anodic electrode potentials and it is concluded that the significant proportion of cathodic activity occurs on the metal surface outside the pit mouth.

Figure 6 shows the solution chemistry in a cavity with corroding walls and base, at a potential of -0.2 V . The same basic trends as for the passive wall case are observed, i.e. increasing chloride and ferrous iron concentration and decreasing pH towards

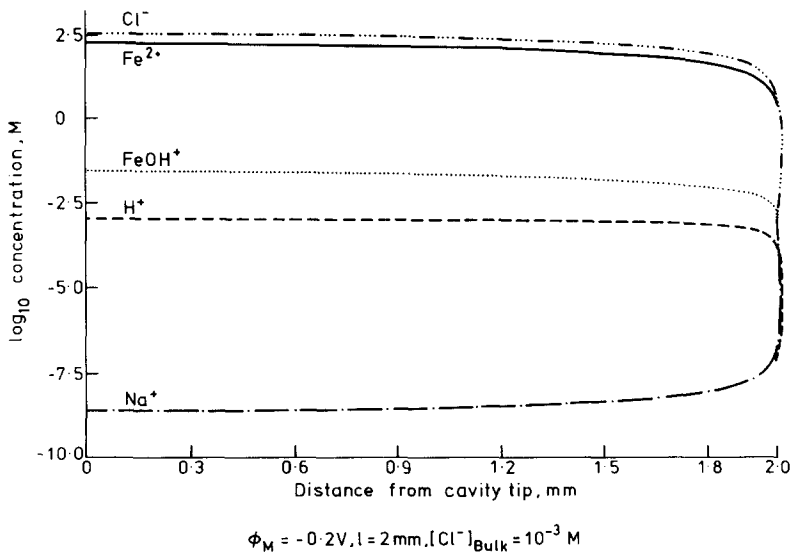


FIG. 6. Concentration profiles along the cavity length for a crevice with corroding walls.

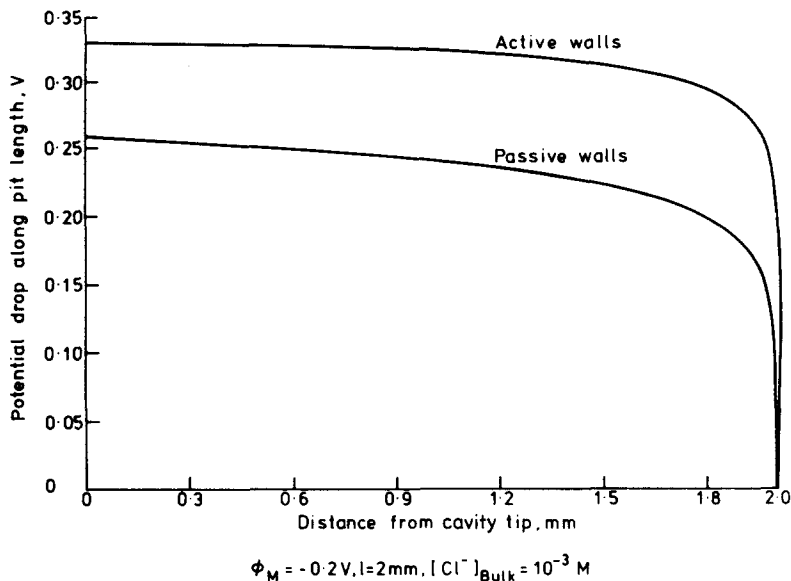


FIG. 7. Comparison of the potential drops along the crevice length for corroding and non-corroding walls.

the cavity tip. The magnitudes of the deviations from bulk values, however, are slightly larger with corroding walls. For example, the pH value at the cavity tip is about 3 compared with 3.4 for the passive walls. The profiles also show more rapid variation near the pit mouth. A comparison of the potential drops for active and passive walls in Fig. 7 indicates that the corrosion currents are reduced when metal dissolution occurs over a larger area. In this case the corrosion current at the pit base is approximately $2 \times 10^2 \text{ A m}^{-2}$ compared with $3 \times 10^3 \text{ A m}^{-2}$ for the passive walls. These currents are still physically unrealistic and a number of other phenomena need to be considered. One important addition is the precipitation of solid ferrous hydroxide, since in all the examples given the solubility limit is exceeded. It will be shown that constraining the ratio of pH value to FeOH^+ reduces the corrosion currents slightly and scaling down the diffusion coefficients to simulate the presence of solid hydroxide reduces them further to physically realistic values.

Passivation of crevice walls

The potential drop along the crevice length can be used to calculate the current distribution over the internal metal surface. Figure 8 shows the corrosion current as a function of position in a cavity of length 2 mm at a potential -0.2 V . The current at the cavity mouth is extremely large, but the model does not account for any passivation of the metal. In reality, it seems likely that this region would repassivate¹ under conditions of higher pH value and lower potential drop in this region. Although the predicted currents in the rest of the cavity are unrealistically high the distribution gives an indication of the future shape of the pit; the rapid broadening of the width close to the mouth with a more even broadening over the majority of the length suggests an eventual bottle-shaped cavity. Most of the current distributions generated for the range of parameters in this paper display this studied behaviour.

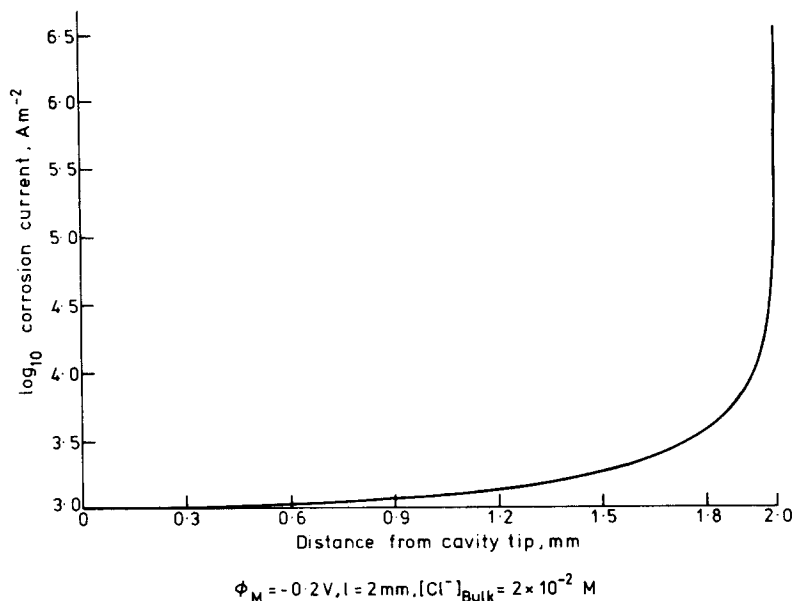
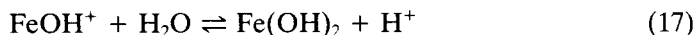


FIG. 8. Corrosion current against cavity length for a crevice with active walls.

PRECIPITATION OF FERROUS HYDROXIDE

In all the examples given in earlier sections the products of ferrous and hydroxide ions have exceeded the solubility limit of solid ferrous hydroxide. As a next stage in the model therefore, the reaction



is considered specifically. The equilibrium constant of this reaction is calculated from the free energies of the individual species as before. In a recent paper, Gravano and Galvele⁶ treat the solid as a diffusing species. They include a term $D(dC/dx)$ directly in their mass-balance equations and solve for this solid 'concentration', C in the same way as for the other concentrations. The diffusion coefficient, D is set to $1 \times 10^{-9} \text{ m}^2 \text{ s}$, the same as the other diffusing ions (except H^+ and OH^-). This describes the situation in the pit a few milliseconds after a flaw in the passive film occurs and assumes that the hydroxide is precipitated as colloidal particles in the very early stages of the process. The model described here considers the effects of precipitation in the crevice over a longer timescale. It does not directly solve for a solid concentration and hence avoids the necessity to assign a diffusion coefficient to a potentially non-mobile species.

There is little kinetic data available on the rate of precipitation. Galvele⁵ suggests in his one-dimensional passive-wall model that no precipitate particles will form along the crevice in the oxide film, as the precipitation process is slow, but at the metal-solution interface the process will be much faster. For simplicity, it will be assumed in this model that the precipitation rate is fast everywhere compared to the diffusion rates and the mass-balance equations will be modified so that the solubility of $\text{Fe}(\text{OH})_2$ is not exceeded.

The governing mass-transport equations are derived as before but with an

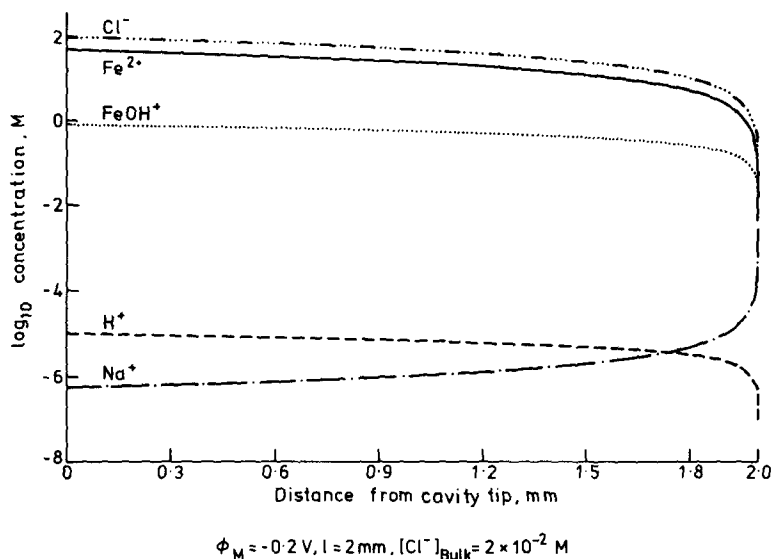


Fig. 9. Concentration profiles along the cavity length for a crevice with passive walls (with a precipitation reaction included but no change to diffusion coefficients).

additional constraint fixing the ratio of the H^+ and FeOH^+ concentrations. The boundary conditions at the pit mouth are modified slightly to ensure both charge neutrality and chemical equilibrium here. The details of the modified equations and boundary conditions may be found in the accompanying paper. The equations are solved using the iteration techniques employed earlier. Figure 9 shows the predicted solution chemistry in a pit with non-corroding walls. The parameters are the same as in the previous calculations except that the bulk chloride concentration is assumed $2 \times 10^{-2} \text{ M}$. The diffusion coefficients are assumed $10^{-9} \text{ m}^2 \text{ s}^{-1}$ (except those of H^+ and OH^-) for this calculation. Comparison of Fig. 9 with a run with the solubility limits exceeded shows a much lesser degree of acidification, about pH 5 at the cavity tip compared with pH 3 (and a correspondingly lower $[\text{FeOH}^+]$). However, the potential distributions in the crevices are very similar and the corrosion currents are only reduced by a few per cent by constraining the pH and FeOH^+ in this way. Figure 10 shows the results of the 'active-wall' calculation using the same parameters as in Fig. 9. Again, it may be seen that the solution is more acidic when the crevice walls are corroding in addition to the base.

In all the examples given the predicted rates of metal dissolution i_1 , are very large. However, no account has been taken of the physical effect of the corrosion product restricting the migration of aqueous species. There are little available empirical data on the diffusion coefficients in porous iron solids, so the model is tested over a range of values. Figure 11 shows the variation of the corrosion currents with diffusion coefficients for the case of an active wall cavity. The reduction in the corrosion current is quite significant as the diffusion of both aggressive species and corrosion products becomes impaired. Figure 12 shows the solution chemistry with a diffusion coefficient of $10^{-13} \text{ m}^2 \text{ s}^{-1}$. Comparison with Fig. 10 shows a higher degree of acidification is obtained since the hydrogen ions produced in the hydrolysis reaction cannot diffuse out of the pit as easily.

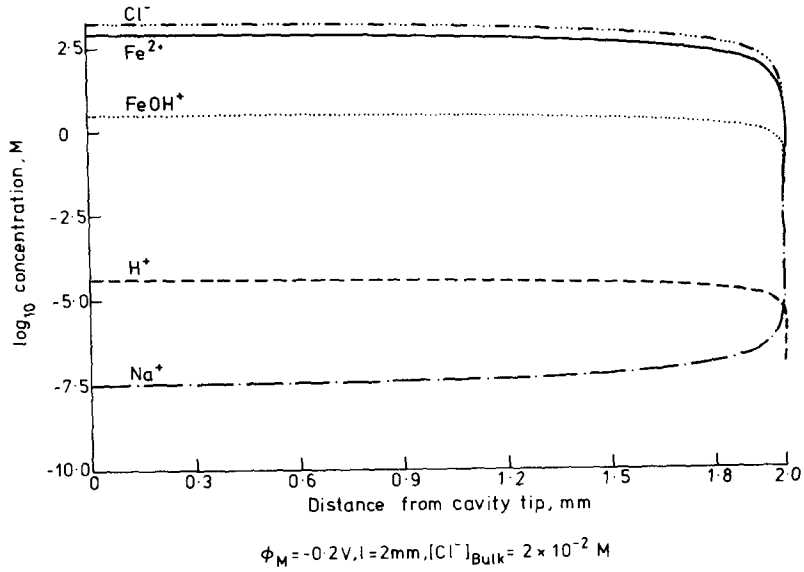


FIG. 10. Concentration profiles along the cavity length for a crevice with active walls (with a precipitation reaction but no change to diffusion coefficients).

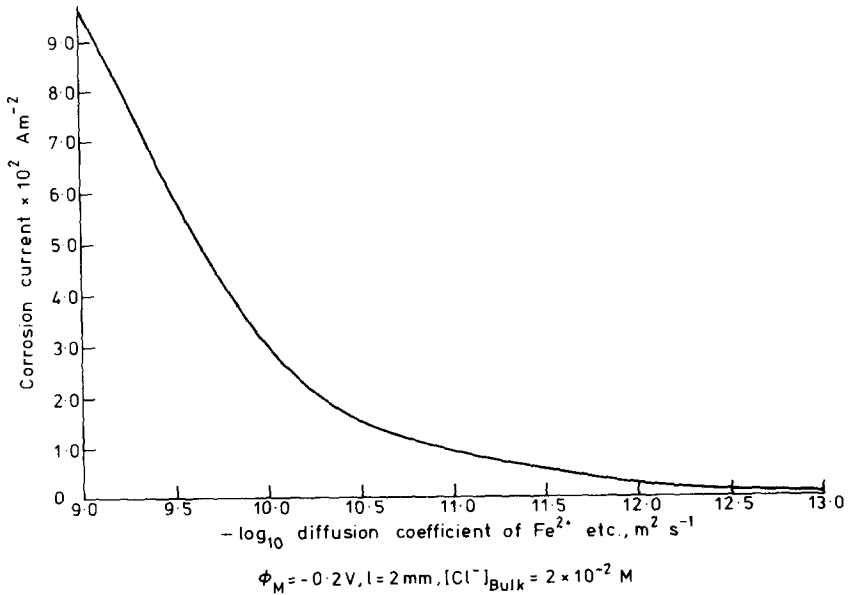


FIG. 11. Corrosion current against diffusion coefficient of Fe²⁺, FeOH⁺, Na⁺ and Cl⁻ for a crevice with active walls.

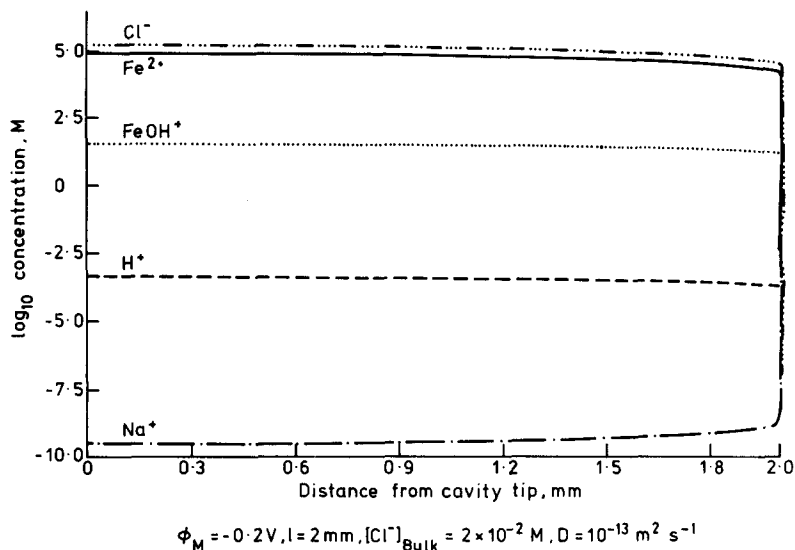


FIG. 12. Concentration profiles along cavity length for a crevice with active walls (precipitation reaction included and diffusion coefficients reduced).

LIMITATIONS AND FUTURE EXTENSIONS TO THE MODEL

The steady-state model described in this paper gives some reasonable qualitative predictions of the chemistry and electrochemistry within the corroding crevice but the quantitative comparisons with empirical cavity propagation rates and ionic concentrations are less encouraging.¹ The inaccurate cavity propagation rates predicted, however, seem consistent with other models in the literature. This would suggest that the approximations made in the construction of the model are not strictly valid and that physical processes have been oversimplified or the empirical input data is not sufficiently accurate. In many of the examples, the predicted solutions are highly supersaturated with respect to ferrous chloride. The addition of the equilibria reaction



would seem necessary in these cases. However, limitations with the numerical solving method of the mass-conservation equations restrict the addition of further chemical equilibria reactions. There is therefore a need to develop an alternative solving technique in the model to include a more complex description of the chemistry within the crevice.

In most of the examples given, the effect of the moving boundary is negligible and the approximation of a static geometry is valid for a steady-state calculation. However, at a high potential, e.g. 0.0 V in pits with passive walls, the calculations produce currents of the order of 10^5 A m^{-2} which is roughly equivalent to the metal interface retreating at a speed of $1 \times 10^{-2} \text{ mm s}^{-1}$. This is fast compared with the diffusive speed of the mobile species and consequently the moving boundary and the induced electrolyte motion should be specifically considered for such sets of parameters.

Another possible extension of the model may be a consideration of the effect of limiting the cathodic current generated on the external surface. Also the electrical resistance of the bulk solution, which modifies the charge transfer and may limit the corrosion rates, should be taken into account.

CONCLUSION

A model of the propagation stage of crevice or pitting corrosion which is entirely predictive and self-consistent is developed and applied to carbon steel in a dilute sodium chloride solution. The steady-state equations governing mass transport and electrode potential of a system of mobile species in a restricted geometry are solved to produce details of variations in the solution chemistry and electrochemical potential. From these results corrosion rates are calculated. The model considers separately active corrosion at the crevice base only and corrosion on the base and walls. An extension to the model includes an account of the effect of precipitation of solid ferrous hydroxide. The main conclusions are as follows:

(1) For both active and passive walls, the results show decreasing pH values and increasing Fe^{2+} and Cl^- concentrations along the pit towards the tip, with deviations of individual species from their bulk values increasing with increasing metal potential. By varying the many parameters of the system it would be possible to identify critical physical conditions (e.g. bulk pH, bulk Cl^- concentration) which result in pitting or crevice corrosion.

(2) In the simplest model, with no solid corrosion products, the calculated corrosion currents for the passive wall case are very high (for $\phi_M = -0.2 \text{ V}$, $l = 2 \text{ mm}$, $i \approx 3 \times 10^3 \text{ A m}^{-2}$) but are reduced by the inclusion of corroding walls ($i \approx 2 \times 10^2 \text{ A m}^{-2}$). When account is taken of the effect of a solid precipitate (ferrous hydroxide) on the solution chemistry, the predicted currents are reduced slightly. However, these values are unrealistically high which would suggest that some of the approximations made in the construction of the model may not be valid. The description of the solution chemistry may still have been over simplified, particularly in the treatment of the solid precipitates. For example, the predicted steady-state solutions within the crevice are highly supersaturated with respect to ferrous chloride. Further model development is necessary to investigate this effect.

(3) The solid corrosion products have an extremely important effect on the cavity propagation rates through their limiting effect on the diffusion ionic species within the crevice. There is little available empirical data on diffusion coefficients within porous iron solids at present and this may be one of the input parameters that needs to be accurately determined if the model is to be used in a predictive role in the future.

(4) For the range of metal potentials considered (-0.4 – 0.0 V) the significant part of cathodic activity occurs on the metal surface outside the crevice mouth.

(5) By considering the proportion of the crevice length at which the potential exceeds the passivation potential of the metal in the crevice solution, i.e. the narrow region near the cavity mouth which does not corrode in the steady state, one could estimate the eventual shape of the crevice. The model predicts a rapid broadening of the width close to the passivated region with a more even broadening and lengthening over the majority of the length. This would suggest an eventual 'bottle-shaped' crevice.

The model will be developed further to include a better description of the solution chemistry in the crevice.

Acknowledgements—This work was jointly funded by the Department of the Environment (DoE) as part of its radioactive waste management research programme, and the Commission of the European Communities. In the DoE context, the results will be used in the formulation of Government policy, but at this stage do not necessarily represent Government policy.

REFERENCES

1. G. P. MARSH, K. J. TAYLOR, I. D. BLAND, C. WESTCOTT, P. W. TASKER and S. M. SHARLAND, *Proc. MRS Symp. Scientific Basis for Nuclear Waste Management*, Stockholm, Sweden (Edited by L. WERNE, p. 421) (Sept. 1985).
2. A. TURNBULL and J. G. N. THOMAS, NPL DMA Report (A), 11 (1979).
3. A. TURNBULL and J. G. N. THOMAS, NPL DMA Report (A), 23 (1980).
4. J. R. GALVELE, *J. Electrochem. Soc.* **123**, 1438 (1976)
5. J. R. GALVELE, *Corros. Sci.* **21**, 551 (1981).
6. S. M. GRAVANO and J. R. GALVELE, *Corros. Sci.* **24**, 517 (1984).
7. A. TURNBULL, *Br. Corros. J.* **15**, 162 (1980).
8. A. TURNBULL and M. R. GARDNER, *Corros. Sci.* **22**, 661 (1982).
9. S. M. SHARLAND, *Corros. Sci.* **28**, 621 (1988).